



**HAL**  
open science

## Synthesis of $\text{Er}_5(\text{BO}_3)_2\text{F}_9$ and Properties of $\text{RE}_5(\text{BO}_3)_2\text{F}_9$ (RE = Er, Yb)

Hubert Huppertz, Almut Haberer, Reinhard Kaindl, Jürgen Konzett, Robert  
Glaum

► **To cite this version:**

Hubert Huppertz, Almut Haberer, Reinhard Kaindl, Jürgen Konzett, Robert Glaum. Synthesis of  $\text{Er}_5(\text{BO}_3)_2\text{F}_9$  and Properties of  $\text{RE}_5(\text{BO}_3)_2\text{F}_9$  (RE = Er, Yb). *Journal of Inorganic and General Chemistry / Zeitschrift für anorganische und allgemeine Chemie*, 2010, 636 (7), pp.1326. 10.1002/zaac.201000085 . hal-00599859

**HAL Id: hal-00599859**

**<https://hal.science/hal-00599859>**

Submitted on 11 Jun 2011

**HAL** is a multi-disciplinary open access archive for the deposit and dissemination of scientific research documents, whether they are published or not. The documents may come from teaching and research institutions in France or abroad, or from public or private research centers.

L'archive ouverte pluridisciplinaire **HAL**, est destinée au dépôt et à la diffusion de documents scientifiques de niveau recherche, publiés ou non, émanant des établissements d'enseignement et de recherche français ou étrangers, des laboratoires publics ou privés.



**Synthesis of Er<sub>5</sub>(BO<sub>3</sub>)<sub>2</sub>F<sub>9</sub> and Properties of RE<sub>5</sub>(BO<sub>3</sub>)<sub>2</sub>F<sub>9</sub>  
(RE = Er, Yb)**

Journal:	<i>Zeitschrift für Anorganische und Allgemeine Chemie</i>
Manuscript ID:	zaac.201000085.R1
Wiley - Manuscript type:	Article
Date Submitted by the Author:	09-Mar-2010
Complete List of Authors:	Huppertz, Hubert; Leopold-Franzens-Universitaet Innsbruck, Institut fuer Allgemeine, Anorganische und Theoretische Chemie Haberer, Almut; Leopold-Franzens-Universitaet Innsbruck, Institut fuer Allgemeine, Anorganische und Theoretische Chemie Kaindl, Reinhard; Leopold-Franzens-Universitaet Innsbruck, Institut für Mineralogie und Petrographie Konzett, Jürgen; Leopold-Franzens-Universitaet Innsbruck, Institut für Mineralogie und Petrographie Glaum, Robert; Universität Bonn, Institut für Anorganische Chemie
Keywords:	Erbium fluoride oxide, High-pressure, Crystal structure



## ARTICLE

DOI: 10.1002/zaac.200((will be filled in by the editorial staff))

Synthesis of  $\text{Er}_5(\text{BO}_3)_2\text{F}_9$  and Properties of  $\text{RE}_5(\text{BO}_3)_2\text{F}_9$  ( $\text{RE} = \text{Er}, \text{Yb}$ )Almut Haberer<sup>[a]</sup>, Reinhard Kaindl<sup>[b]</sup>, Jürgen Konzett<sup>[b]</sup>, Robert Glaum<sup>[c]</sup>, and Hubert Huppertz<sup>\*[a]</sup>*Dedicated to Professor Rüdiger Kniep on the Occasion of His 65<sup>th</sup> Birthday***Keywords:** Erbium fluoride oxide; High-pressure; Crystal structure

$\text{Er}_5(\text{BO}_3)_2\text{F}_9$  was synthesized under conditions of 3 GPa and 800 °C in a Walker-type multianvil apparatus. The crystal structure was determined on the basis of single-crystal X-ray diffraction data, collected at room temperature.  $\text{Er}_5(\text{BO}_3)_2\text{F}_9$  is isotypic to the recently synthesized  $\text{Yb}_5(\text{BO}_3)_2\text{F}_9$  and crystallizes in  $C2/c$  with the lattice parameters  $a = 2031.2(4)$  pm,  $b = 609.5(2)$  pm,  $c = 824.6(2)$  pm, and  $\beta = 100.29(3)^\circ$ . The physical properties of  $\text{RE}_5(\text{BO}_3)_2\text{F}_9$  ( $\text{RE} = \text{Er}, \text{Yb}$ ) including high temperature behaviour and single crystal IR- / Raman spectroscopy were investigated.

\* Univ.-Prof. Dr. Hubert Huppertz

Email: Hubert.Huppertz@uibk.ac.at

[a] Institut für Allgemeine, Anorganische und Theoretische

Chemie

Leopold-Franzens-Universität Innsbruck

Innrain 52a

6020 Innsbruck, Austria

[b] Institut für Mineralogie und Petrographie

Leopold-Franzens-Universität Innsbruck

Innrain 52

6020 Innsbruck, Austria

[c] Institut für Anorganische Chemie

Universität Bonn

Gerhard-Domagk-Str. 1

53121 Bonn, Germany

*E.g.*, during our studies of high-pressure phases of the rare-earth borates, the compounds  $\text{RE}_4\text{B}_6\text{O}_{15}$  ( $\text{RE} = \text{Dy}, \text{Ho}$ ) [6-8] were intensively investigated. Nevertheless, it was not possible to obtain isotypical compounds with  $\text{RE} = \text{Er}, \text{Tm}, \text{Yb},$  or  $\text{Lu}$ . For these rare-earth elements, high-pressure / high-temperature experiments always yielded the compounds  $\text{RE}_3\text{B}_5\text{O}_{12}$  ( $\text{RE} = \text{Er-Lu}$ ) [9].

In analogy to these investigations of the rare-earth borates, we are trying to define the formation region for the composition  $\text{RE}_5(\text{BO}_3)_2\text{F}_9$ . While  $\text{Yb}_5(\text{BO}_3)_2\text{F}_9$  was synthesized at 7.5 GPa [1], an isotypic erbium fluoride borate  $\text{Er}_5(\text{BO}_3)_2\text{F}_9$  could be obtained now at a pressure of 3 GPa. This indicates that there is a large pressure region for the formation of these high-pressure phases and the application of similar synthetic conditions to neighbouring rare-earth elements could thus lead to additional isotypic compounds. Since it was possible to obtain  $\text{Er}_5(\text{BO}_3)_2\text{F}_9$ , the existence of an isotypic thulium compound is more than likely. Future studies will show, if the synthesis with larger rare-earth cations is possible as well and at which point we observe the formation of another structure type as in the borate case. However, experiments on  $\text{Yb}_5(\text{BO}_3)_2\text{F}_9$  at higher pressures (10 GPa) resulted already in the formation of an apatite-structured compound, wherein all boron atoms showed a fourfold coordination [10].

In this paper, we present the synthesis and structural details of  $\text{Er}_5(\text{BO}_3)_2\text{F}_9$  in comparison to the isotypic phase  $\text{Yb}_5(\text{BO}_3)_2\text{F}_9$ . Furthermore, several physical properties of the compounds  $\text{RE}_5(\text{BO}_3)_2\text{F}_9$  ( $\text{RE} = \text{Er}, \text{Yb}$ ) are reported.

**Experimental Section**

To synthesize the compound  $\text{Er}_5(\text{BO}_3)_2\text{F}_9$ , high-pressure / high-temperature conditions of 3 GPa and 800 °C were applied, starting from  $\text{Er}_2\text{O}_3$  (Strem Chemicals, 99.9%),  $\text{B}_2\text{O}_3$  (Strem Chemicals, 99.9+%), and  $\text{ErF}_3$  (Strem Chemicals, 99.+%) at equal molar ratios. The starting materials were ground up and filled into a boron nitride crucible (Henze BNP GmbH, HeBoSint® S100, Kempten,

**Introduction**

In the past years, the field of rare-earth fluorido- and fluoride borates could be greatly extended by the application of high-pressure / high-temperature techniques, leading to the new compounds  $\text{Yb}_5(\text{BO}_3)_2\text{F}_9$  [1],  $\text{Pr}_4\text{B}_3\text{O}_{10}\text{F}$  [2], and  $\text{Gd}_4\text{B}_4\text{O}_{11}\text{F}_2$  [3].

Before we started our high-pressure / high-temperature research, rare-earth fluorido- and fluoride borates were only represented by the compounds  $\text{RE}_3(\text{BO}_3)_2\text{F}_3$  ( $\text{RE} = \text{Sm}, \text{Eu}, \text{Gd}$ ) [4] and  $\text{Gd}_2(\text{BO}_3)\text{F}_3$  [5], synthesized by heating a stoichiometric mixture of  $\text{RE}_2\text{O}_3$ ,  $\text{B}_2\text{O}_3$ , and  $\text{REF}_3$  under ambient pressure conditions. There is a close relationship between these two structure-types and the recently discovered high-pressure ytterbium fluoride borate  $\text{Yb}_5(\text{BO}_3)_2\text{F}_9$  [1]. All three compounds can be described *via* alternating layers of the formal compositions “ $\text{REBO}_3$ ” and “ $\text{REF}_3$ ” in the  $bc$ -plane. It should be emphasized that the crystal structures of the actual compounds  $\text{REBO}_3$  and  $\text{REF}_3$  can not be compared with the structures of the layers, so that “ $\text{REBO}_3$ ” and “ $\text{REF}_3$ ” only stand for the formal composition of the layers. We are now trying to substitute the  $\text{Yb}^{3+}$  ions of  $\text{Yb}_5(\text{BO}_3)_2\text{F}_9$  with other rare-earth cations to yield isotypic  $\text{RE}_5(\text{BO}_3)_2\text{F}_9$  phases, different structures, or new compositions dependent of the size of the rare-earth ion.

Germany). The compounds were compressed and heated *via* a multianvil assembly, based on a Walker-type module and a 1000 ton press (both devices from the company Voggenreiter, Mainleus, Germany). Eight tungsten carbide cubes (TSM-20, Ceratizit, Reutte, Austria) compressed the boron nitride crucible, which was positioned inside the centre of an 18/11 assembly. A detailed description of the assembly can be found in reference [11].

The 18/11 assembly was compressed up to 3 GPa in 1.25 h and heated to 800 °C (cylindrical graphite furnace) in the following 10 min, kept there for 20 min, and cooled down to 600 °C in 20 min at constant pressure. After natural cooling down to room temperature by switching off the heating, a decompression period of 3.75 hours was required. Then the recovered octahedral pressure medium (MgO, Ceramic Substrates & Components Ltd., Newport, Isle of Wight, UK) was broken apart and the sample carefully separated from the surrounding graphite and boron nitride. Pink air- and water-resistant crystals of  $\text{Er}_5(\text{BO}_3)_2\text{F}_9$  were obtained.

### Crystal Structure Analysis

The sample was characterized by powder X-ray diffraction, which was performed in transmission geometry on a flat sample of the reaction product, using a STOE STADI P powder diffractometer with  $\text{MoK}_{\alpha 1}$  radiation (Ge monochromator,  $\lambda = 71.073$  pm). The powder pattern showed reflections of  $\text{Er}_5(\text{BO}_3)_2\text{F}_9$  and of  $\mu\text{-ErBO}_3$  [12] as a by-product of the synthesis (Figure 1). The experimental powder pattern tallied well with the theoretical pattern of  $\text{Er}_5(\text{BO}_3)_2\text{F}_9$ , simulated from single-crystal data. Indexing the reflections of the erbium fluoride borate, we got the parameters  $a = 2033.0(3)$  pm,  $b = 610.6(3)$  pm, and  $c = 825.5(4)$  pm, with  $\beta = 100.29(6)^\circ$  and a volume of  $1008.2(9) \text{ \AA}^3$ . This confirmed the lattice parameters, obtained from single-crystal X-ray diffraction (Table 1).

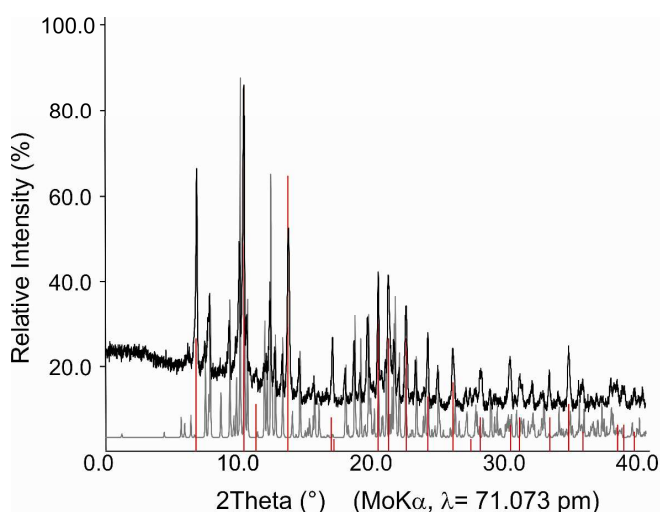


Figure 1. Experimental powder pattern of  $\text{Er}_5(\text{BO}_3)_2\text{F}_9$  in comparison to the theoretical powder pattern beneath, based on single-crystal diffraction data. Reflections of  $\mu\text{-ErBO}_3$  are marked with lines.

Intensity data of a single-crystal of  $\text{Er}_5(\text{BO}_3)_2\text{F}_9$  were collected at room temperature by use of a Kappa CCD diffractometer (Bruker AXS / Nonius, Karlsruhe), equipped with a Miracol Fiber Optics Collimator and a Nonius FR590 generator (graphite-monochromatized  $\text{MoK}_{\alpha 1}$  radiation,  $\lambda = 71.073$  pm). An absorption correction, based on multi-scans [13], was applied to the data set.

All relevant details of the data collection and evaluation are listed in Table 1.

Table 1. Crystal data and structure refinement of  $\text{Er}_5(\text{BO}_3)_2\text{F}_9$

Empirical Formula	$\text{Er}_5(\text{BO}_3)_2\text{F}_9$
Molar mass ( $\text{g}\cdot\text{mol}^{-1}$ )	1124.92
Crystal system	monoclinic
Space group	$C2/c$ (No. 15)
Lattice parameters from powder data	
Powder diffractometer	STOE STADI P
Radiation	$\text{MoK}_{\alpha 1}$ ( $\lambda = 71.073$ pm)
$a$ (pm)	2033.0(3)
$b$ (pm)	610.6(3)
$c$ (pm)	825.5(4)
$\beta$ (deg)	100.29(6)
Volume ( $\text{\AA}^3$ )	1008.2(9)
Single-crystal data	
Single-crystal diffractometer	Bruker AXS / Nonius Kappa CCD
Radiation	$\text{MoK}_{\alpha 1}$ ( $\lambda = 71.073$ pm)
$a$ (pm)	2031.2(4)
$b$ (pm)	609.5(2)
$c$ (pm)	824.6(2)
$\beta$ (deg)	100.29(3)
Volume ( $\text{\AA}^3$ )	1004.4(3)
Formula units per cell	4
Temperature (K)	293(2)
Calculated density ( $\text{g}\cdot\text{cm}^{-3}$ )	7.44
Crystal size ( $\text{mm}^3$ )	$0.03 \times 0.02 \times 0.02$
Absorption coefficient ( $\text{mm}^{-1}$ )	41.49
$F(000)$	1916
$\theta$ range (deg)	$2.0 \leq \theta \leq 37.9$
Range in $hkl$	$-33/34, \pm 10, -14/12$
Total no. reflections	7955
Independent reflections	2700 ( $R_{\text{int}} = 0.0382$ )
Reflections with $I > 2\sigma(I)$	2315 ( $R_{\sigma} = 0.0389$ )
Data / parameters	2700 / 102
Absorption correction	Multi-scan [13]
Goodness-of-fit ( $F^2$ )	1.062
Final $R$ indices ( $I > 2\sigma(I)$ )	$R1 = 0.0289$ $wR2 = 0.0530$
$R$ indices (all data)	$R1 = 0.0384$ $wR2 = 0.0558$
Largest differ. peak / deepest hole ( $\text{e}\cdot\text{\AA}^{-3}$ )	2.71 / -2.55

The structure solution and the parameter refinement (full-matrix least-squares against  $F^2$ ) were successfully performed, using the SHELX-97 software suite [14,15] with anisotropic atomic displacement parameters for all atoms. According to the systematic extinctions, the orthorhombic space groups  $C2/c$  and  $Cc$  were derived. The structure solution in  $C2/c$  (no. 15) succeeded. The final difference Fourier syntheses did not reveal any significant residual peaks in all refinements. The positional parameters of the refinements, anisotropic displacement parameters, interatomic distances, and interatomic angles are listed in the Tables 2-5. Further information of the crystal structure is available from the Fachinformationszentrum Karlsruhe (crysdata@fiz-karlsruhe.de), D-76344 Eggenstein-Leopoldshafen (Germany), by quoting the Registry No. CSD-421469.

Table 2. Atomic coordinates and isotropic equivalent displacement parameters ( $U_{eq} / \text{\AA}^2$ ) for  $\text{Er}_5(\text{BO}_3)_2\text{F}_9$  (space group:  $C2/c$ ). Wyckoff sites are  $4e$  for Er3 and F3 and  $8f$  for all other atoms.  $U_{eq}$  is defined as one-third of the trace of the orthogonalized  $U_{ij}$  tensor.

Atom	x	y	z	$U_{eq}$
Er1	0.30661(2)	0.11935(3)	0.18057(2)	0.00619(5)
Er2	0.39031(2)	0.38886(3)	0.59380(2)	0.00770(5)
Er3	$\frac{1}{2}$	0.11138(5)	$\frac{1}{4}$	0.00783(6)
B1	0.3884(3)	0.902(2)	0.4368(8)	0.014(2)
O1	0.4087(2)	0.7605(6)	0.5638(4)	0.0080(6)
O2	0.3392(2)	0.0678(7)	0.4620(4)	0.0123(7)
O3	0.4082(2)	0.1054(6)	0.7829(4)	0.0081(6)
F1	0.2890(2)	0.4245(5)	0.0195(4)	0.0089(5)
F2	0.3683(2)	0.5761(5)	0.8143(4)	0.0107(5)
F3	$\frac{1}{2}$	0.4892(7)	$\frac{1}{4}$	0.0134(8)
F4	0.2752(2)	0.7781(5)	0.2150(4)	0.0128(6)
F5	0.4693(2)	0.1849(6)	0.5136(5)	0.0192(7)

## Results and Discussion

### Crystal Structure of $\text{Er}_5(\text{BO}_3)_2\text{F}_9$

The structure of  $\text{Er}_5(\text{BO}_3)_2\text{F}_9$  consists of isolated  $\text{BO}_3$ -groups, erbium cations, and fluoride anions (Figure 2). The arrangement can be described *via* alternating layers of the formal compositions “ $\text{ErBO}_3$ ” and “ $\text{ErF}_3$ ”, spreading into the  $bc$ -plane. For a more detailed description of the structure, including a comparison to the related structures of  $\text{RE}_3(\text{BO}_3)_2\text{F}_3$  ( $\text{RE} = \text{Sm}, \text{Eu}, \text{Gd}$ ) [5] and  $\text{Gd}_2(\text{BO}_3)\text{F}_3$  [6], the reader is referred to the description of the isotopic compound  $\text{Yb}_5(\text{BO}_3)_2\text{F}_9$  (ref. [1]). In this paper, we briefly compare the main features of the compounds.

Table 3. Interatomic distances (pm) in  $\text{Er}_5(\text{BO}_3)_2\text{F}_9$ , calculated with the single-crystal lattice parameters.

Er1–O2a	231.8(4)	Er2–O3	231.2(3)	Er3–O1	232.2(4)
Er1–O2b	232.7(4)	Er2–O1	231.6(4)		(2 ×)
Er1–O3	249.6(4)	Er2–O2	238.4(4)	Er3–O3	234.0(3)
Er1–O1	254.5(4)	Er2–F5	222.2(4)		(2 ×)
Er1–F4a	220.9(3)	Er2–F2a	225.8(3)	Er3–F3	230.3(5)
Er1–F4b	222.4(3)	Er2–F2b	227.8(3)	Er3–F5a	240.8(4)
Er1–F1a	227.6(3)	Er2–F1	233.6(3)		(2 ×)
Er1–F1b	232.8(3)	Er2–F3	248.0(2)	Er3–F5b	264.9(4)
Er1–F2	239.6(3)	Er2–F4	288.8(4)		(2 ×)
<hr/>					
B1–O1	136.4(7)				
B1–O3	139.8(7)				
B1–O2	146.1(8)	<b><math>\theta = 140.8</math></b>			
<hr/>					
F1–Er1a	227.6(3)	F2–Er2a	225.8(3)	F3–Er3	230.3(5)
F1–Er2	233.6(3)	F2–Er2b	227.8(3)	F3–Er2	248.0(2)
F1–Er1b	232.8(3)	F2–Er1	239.6(3)		(2 ×)
<hr/>					
F4–Er1a	220.9(3)	F5–Er2	222.2(4)		
F4–Er1b	222.4(3)	F5–Er3a	239.2(5)		
F4–Er2	288.8(4)	F5–Er3b	264.9(4)		

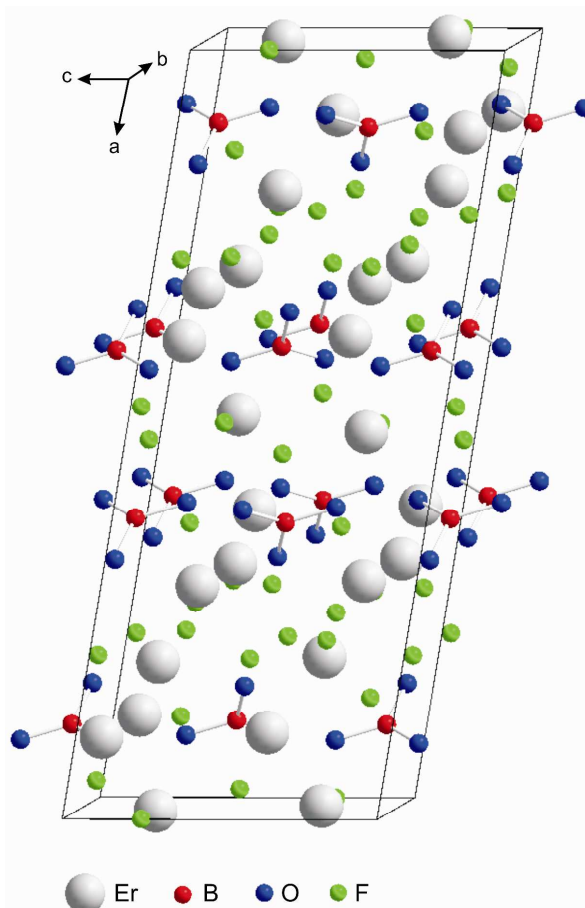


Figure 2. Crystal structure of  $\text{Er}_5(\text{BO}_3)_2\text{F}_9$ , showing isolated  $\text{BO}_3$ -groups.

With  $a = 2031.4(2)$  pm,  $b = 609.5(2)$  pm, and  $c = 824.6(2)$  pm, the lattice parameters of  $\text{Er}_5(\text{BO}_3)_2\text{F}_9$  are slightly larger than those of  $\text{Yb}_5(\text{BO}_3)_2\text{F}_9$  ( $a = 2028.0(2)$ ,  $b = 602.5(3)$ , and  $c = 821.5(5)$  pm). This can be ascribed to the slightly larger size of  $\text{Er}^{3+}$  (ionic radius = 120 pm for a ninefold coordination [16]), compared to  $\text{Yb}^{3+}$  (ionic radius = 118 pm for coordination number nine [16]). Since the size difference is marginally, no greater deviations of the bond lengths and angles are observed. In both compounds, each of the three crystallographically independent rare-earth cations exhibits a coordination number of nine. In  $\text{Er}_5(\text{BO}_3)_2\text{F}_9$ , we find Er–O/F distances in the range of 231.2(3) – 288.8(4) pm, which tally well with the values obtained for the Yb–O/F distances in  $\text{Yb}_5(\text{BO}_3)_2\text{F}_9$  (227.4(5) to 294.2(5) pm). Focussing on the coordination spheres of the fluoride ions, we find a coordination number of three for all fluoride ions in the two isotopic compounds. In  $\text{Yb}_5(\text{BO}_3)_2\text{F}_9$ , the F–Yb distances are slightly shorter than the F–Er bond lengths in  $\text{Er}_5(\text{BO}_3)_2\text{F}_9$ , which agrees with the slight size difference of the cations.

Inside the  $\text{BO}_3$ -groups, the B–O distances of  $\text{Er}_5(\text{BO}_3)_2\text{F}_9$  vary between 136.4(7) and 146.1(8) pm (Table 3). The B–O bond lengths tally with those in  $\text{Yb}_5(\text{BO}_3)_2\text{F}_9$  (between 138.7(10) and 148.0(12) pm). The unusually large B–O2 bond of 148 pm, observed in  $\text{Yb}_5(\text{BO}_3)_2\text{F}_9$ , is slightly shorter in the erbium compound (146.1(8) pm), but still exceeds typical bond lengths in  $\text{BO}_3$ -groups, which are

usually in a range around 137 pm, *e.g.* in borates with a calcite structure (AlBO<sub>3</sub> (137.96(4) pm) [17],  $\beta$ -YbBO<sub>3</sub> (137.8(4) pm) [18], and FeBO<sub>3</sub> (137.9(2) pm) [19]).

Table 4. Interatomic angles (deg) in Er<sub>5</sub>(BO<sub>3</sub>)<sub>2</sub>F<sub>9</sub>, calculated with the single-crystal lattice parameters.

O1–B1–O3	125.4(5)	Er1a–F1–Er2	101.9(2)
O1–B1–O2	116.7(5)	Er1a–F1–Er1b	110.1(2)
O3–B1–O2	117.9(5)	Er2–F1–Er1b	145.7(2)
	<b><math>\bar{\theta} = 120.0</math></b>		<b><math>\bar{\theta} = 119.2</math></b>
Er2a–F2–Er2b	146.2(2)	Er3–F3–Er2a	107.4(2)
Er2a–F2–Er1	100.6(2)	Er3–F3–Er2b	107.4(2)
Er2b–F2–Er1	112.6(2)	Er2a–F3–Er2b	145.1(2)
	<b><math>\bar{\theta} = 119.8</math></b>		<b><math>\bar{\theta} = 120.0</math></b>
Er1a–F4–Er1b	135.4(2)	Er2–F5–Er3a	133.6(2)
Er1a–F4–Er2	91.0(2)	Er2–F5–Er3b	104.5(2)
Er1b–F4–Er2	133.4(2)	Er3a–F5–Er3b	118.2(2)
	<b><math>\bar{\theta} = 199.9</math></b>		<b><math>\bar{\theta} = 118.8</math></b>

In analogy to Yb<sub>5</sub>(BO<sub>3</sub>)<sub>2</sub>F<sub>9</sub>, we have calculated the charge distribution of the atoms in Er<sub>5</sub>(BO<sub>3</sub>)<sub>2</sub>F<sub>9</sub> *via* bond valence sums ( $\Sigma V$ ) with VaList (Bond Valence Calculation and Listing) [20] and with the CHARDI concept ( $\Sigma Q$ ) [21–23], confirming the formal valence states in the fluoride borate. Table 5 displays the results of the formal ionic charges of the atoms, which are in agreement within the limits of both concepts. In Yb<sub>5</sub>(BO<sub>3</sub>)<sub>2</sub>F<sub>9</sub>, the bond valence sums for the boron atom were extraordinarily low ( $\Sigma V = 2.59$ ), due to the large B–O2 bond present in the structure. Since the boron bond lengths are shorter in Er<sub>5</sub>(BO<sub>3</sub>)<sub>2</sub>F<sub>9</sub>, we now obtain a better value of  $\Sigma V = 2.73$  for B1. Furthermore, we have calculated the MAPLE value (*Madelung Part of Lattice Energy* according to Hoppe [24–26]) of Er<sub>5</sub>(BO<sub>3</sub>)<sub>2</sub>F<sub>9</sub> to compare it with the sum of the MAPLE values for the underlying binary components, namely the high-pressure modification of Er<sub>2</sub>O<sub>3</sub> [27], the ambient-pressure modification of B<sub>2</sub>O<sub>3</sub> (B<sub>2</sub>O<sub>3</sub>–I) [28], and ErF<sub>3</sub> [29]. We obtained a value of 53879 kJ/mol in comparison to 53240 kJ/mol (deviation: 1.2 %), starting from the binary components [1 × Er<sub>2</sub>O<sub>3</sub> (15283 kJ/mol) + 1 × B<sub>2</sub>O<sub>3</sub>–I (20626 kJ/mol) + 3 × ErF<sub>3</sub> (17331 kJ/mol)].

Table 5. Charge distribution in Er<sub>5</sub>(BO<sub>3</sub>)<sub>2</sub>F<sub>9</sub>, calculated with VaList ( $\Sigma V$ ) [20] and the CHARDI concept ( $\Sigma Q$ ) [21–23].

	Er1	Er2	Er3	B1
$\Sigma V$	3.09	2.94	2.70	2.73
$\Sigma Q$	3.06	2.92	3.05	3.00
	O1	O2	O3	F1
$\Sigma V$	-2.06	-1.94	-1.99	-0.96
$\Sigma Q$	-2.20	-1.80	-1.95	-1.10
	F2	F3	F4	F5
$\Sigma V$	-1.01	-0.76	-0.93	-0.81
$\Sigma Q$	-1.14	-0.88	-0.91	-0.95

### Elemental analyses

Since it is nearly impossible to distinguish between fluoride ions and hydroxyl groups by means of electron density or bond lengths, we performed elemental analyses on our samples of RE<sub>5</sub>(BO<sub>3</sub>)<sub>2</sub>F<sub>9</sub> (RE = Er, Yb) to assure the atom assignments in both structures. EDX measurements were performed on a JEOL JSM-6500F scanning electron microscope, equipped with a field emission gun at an acceleration voltage of 16 kV. Samples were prepared by placing single crystals of both phases on adhesive conductive pads and subsequently coating them with a thin conductive carbon film. Each EDX spectrum (Oxford Instruments) was recorded with the analyzed area limited on one single crystal to avoid the influence of possibly contaminating phases. The crystals of Er<sub>5</sub>(BO<sub>3</sub>)<sub>2</sub>F<sub>9</sub> showed average atomic compositions (theoretical values in brackets) of Er 63.1 (74.3) wt%; B 8.9 (1.9) wt%; O 9.3 (8.5) wt%; F 18.7 (15.2) wt%. For Yb<sub>5</sub>(BO<sub>3</sub>)<sub>2</sub>F<sub>9</sub>, average compositions (wt%) of Yb 70.7 (75.0) wt%; B 4.6 (1.9) wt%; O 8.4 (8.3) wt%; F 16.3 (14.8) wt% were obtained. Due to the light weight of boron, measurements have to be taken with caution, but still, these results confirm the presence of all elements and the composition, obtained from the single crystal structure determination.

Furthermore, the composition of Yb<sub>5</sub>(BO<sub>3</sub>)<sub>2</sub>F<sub>9</sub> was confirmed by chemical analysis with a JEOL JXA-8100 electron microprobe. The sample was prepared by embedding bulk material in epoxy resin and polishing with diamond polishing paste. Analytical conditions were a 15 kV acceleration voltage and a 20 nA beam current with measurement times of 40 sec on the peaks and 20 sec on the backgrounds of the O-K $\alpha$ , F-K $\alpha$ , and Yb-L $\alpha$  X-ray lines. SiO<sub>2</sub>, Al<sub>2</sub>SiO<sub>4</sub>F<sub>2</sub>, and Yb<sub>5</sub>P<sub>5</sub>O<sub>14</sub> were used as standards for O, F, and Yb, respectively, and the raw counts were corrected with the ZAF correction procedure. Boron could not be determined quantitatively with the electron microprobe due to its low concentration. An average of 3 analyses on three different crystals yielded (theoretical values in brackets): Yb 74.4±0.2 (75.0) wt%; O 8.6±0.4 (8.3) wt%; F 14.5±0.6 (14.8) wt%.

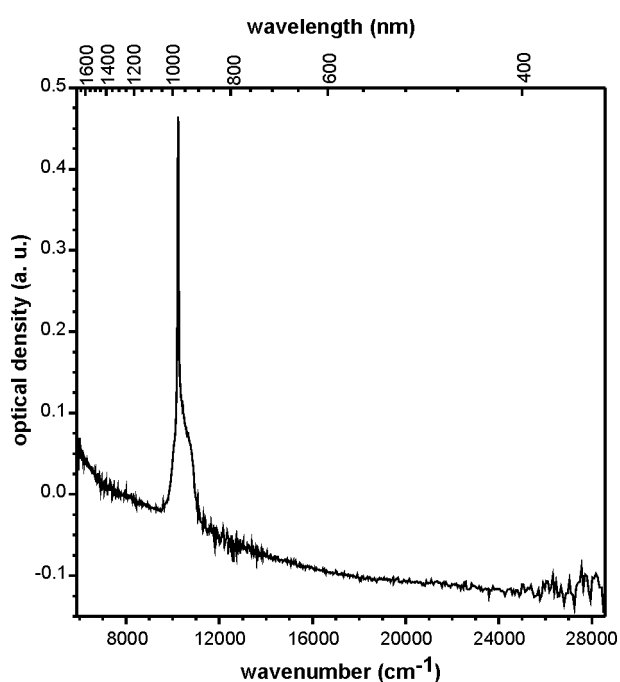
### Physical Properties of RE<sub>5</sub>(BO<sub>3</sub>)<sub>2</sub>F<sub>9</sub> (RE = Er, Yb)

#### UV/vis spectroscopy of Yb<sub>5</sub>(BO<sub>3</sub>)<sub>2</sub>F<sub>9</sub>

The electronic absorption spectrum of Yb<sub>5</sub>(BO<sub>3</sub>)<sub>2</sub>F<sub>9</sub> was measured at 293 K in the nir/vis/UV (5800 – 28000 cm<sup>-1</sup>, step-width  $\Delta\lambda(\text{UV/vis}) = 1 \text{ nm}$ ,  $\Delta\lambda(\text{nir}) = 2 \text{ nm}$ ), using a strongly modified CARY 17 microcrystal spectrophotometer (Spectra Services, ANU Canberra, Australia). Details of the spectrometer have already been described in literature [30, 31]. A polycrystalline agglomerate with dimensions 0.2 × 0.2 × 0.05 mm<sup>3</sup> was selected for the investigation. The noisy spectrum (Fig. 3) results from the small size and rather modest optical quality of the agglomerate. The reference intensity was measured with a pinhole instead of the crystal mounted on an aperture. The electronic absorption spectrum of a polycrystalline agglomerate of Yb<sub>5</sub>(BO<sub>3</sub>)<sub>2</sub>F<sub>9</sub> shows the transition <sup>2</sup>F<sub>7/2</sub> → <sup>2</sup>F<sub>5/2</sub>, expected for Yb<sup>3+</sup> at  $\tilde{\nu} \approx 10400 \text{ cm}^{-1}$  [32]. Due to weak ligand-field interaction, the signal is split

into a sharp peak at  $\tilde{\nu} = 10236 \text{ cm}^{-1}$  and a broader shoulder at  $\tilde{\nu} = 10660 \text{ cm}^{-1}$ .

Figure 3. Electronic absorption spectrum of a polycrystalline agglomerate of  $\text{Yb}_5(\text{BO}_3)_2\text{F}_9$ .



#### IR spectroscopy

FTIR absorbance spectra of single crystals of  $\text{RE}_5(\text{BO}_3)_2\text{F}_9$  ( $\text{RE} = \text{Er}, \text{Yb}$ ) were measured in transmitted, polarized light on a  $\text{BaF}_2$  plate using a BRUKER VERTEX 70 spectrometer, attached to a HYPERION 3000 microscope, a MIR light source, and a LN-MCT detector. Spectral resolution was  $\sim 4 \text{ cm}^{-1}$ . Minimum-maximum normalization was done by the OPUS 6.5 software (BRUKER). In Figure 4, the spectra of both compounds are displayed. The absorptions of  $\text{Yb}_5(\text{BO}_3)_2\text{F}_9$  (Fig. 4, bottom) correspond to the absorptions measured on the bulk material (Ref. [1]). In the IR-spectrum of the isotopic erbium compound (Fig. 4, top), the absorption bands are slightly shifted to higher wavelengths. The absorption patterns of the IR spectra are typical for borates exhibiting triangular  $\text{BO}_3$ -groups [1, 33, 34]. Below  $600 \text{ cm}^{-1}$  for  $\text{Yb}_5(\text{BO}_3)_2\text{F}_9$  and below  $650 \text{ cm}^{-1}$  for  $\text{Er}_5(\text{BO}_3)_2\text{F}_9$ , bands are evoked by the in plane bending ( $\nu_4$ ) of the  $\text{BO}_3$ -groups. The strong and usually sharp absorptions derived from the out of plane bending ( $\nu_2$ ) of the trigonal ion occur in the range of  $600 - 780 \text{ cm}^{-1}$  for  $\text{Yb}_5(\text{BO}_3)_2\text{F}_9$  and  $650 - 850 \text{ cm}^{-1}$  for  $\text{Er}_5(\text{BO}_3)_2\text{F}_9$ . According to the crystalline environment, the absorption bands between  $800 - 950 \text{ cm}^{-1}$  for  $\text{Yb}_5(\text{BO}_3)_2\text{F}_9$  and  $900 - 1000 \text{ cm}^{-1}$  for  $\text{Er}_5(\text{BO}_3)_2\text{F}_9$  can be classified as symmetric stretching vibrations ( $\nu_1$ ). Asymmetric stretching vibrations ( $\nu_3$ ) of the  $\text{BO}_3$ -groups are assigned in the areas of  $1150 - 1400 \text{ cm}^{-1}$  for  $\text{Yb}_5(\text{BO}_3)_2\text{F}_9$  and of  $1200 - 1500 \text{ cm}^{-1}$  for  $\text{Er}_5(\text{BO}_3)_2\text{F}_9$ . Interestingly, two bands between  $3400$  and  $3600 \text{ cm}^{-1}$  were detected in the single crystal spectra of  $\text{RE}_5(\text{BO}_3)_2\text{F}_9$  ( $\text{RE} = \text{Er}, \text{Yb}$ ) (Figure 5), which were not present in the corresponding spectrum of dried bulk  $\text{Yb}_5(\text{BO}_3)_2\text{F}_9$  [1]. Bands in this range usually indicate OH-groups in water-containing borates. The substitution of fluoride with hydroxyl groups is a problem commonly known from fluoride borates [3, 4].

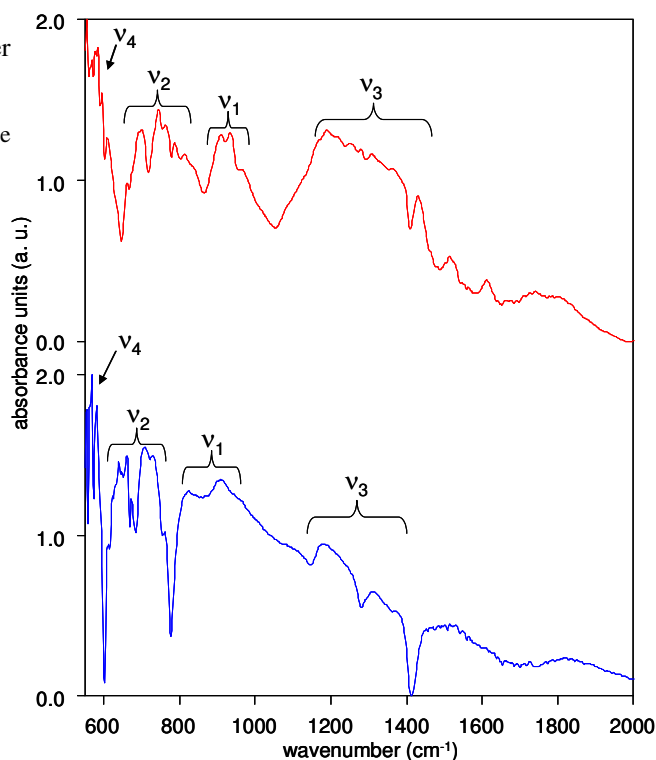


Figure 4. FTIR absorbance spectra of single crystals of  $\text{Er}_5(\text{BO}_3)_2\text{F}_9$  (top) and  $\text{Yb}_5(\text{BO}_3)_2\text{F}_9$  (bottom) in the range  $550\text{-}2000 \text{ cm}^{-1}$ .

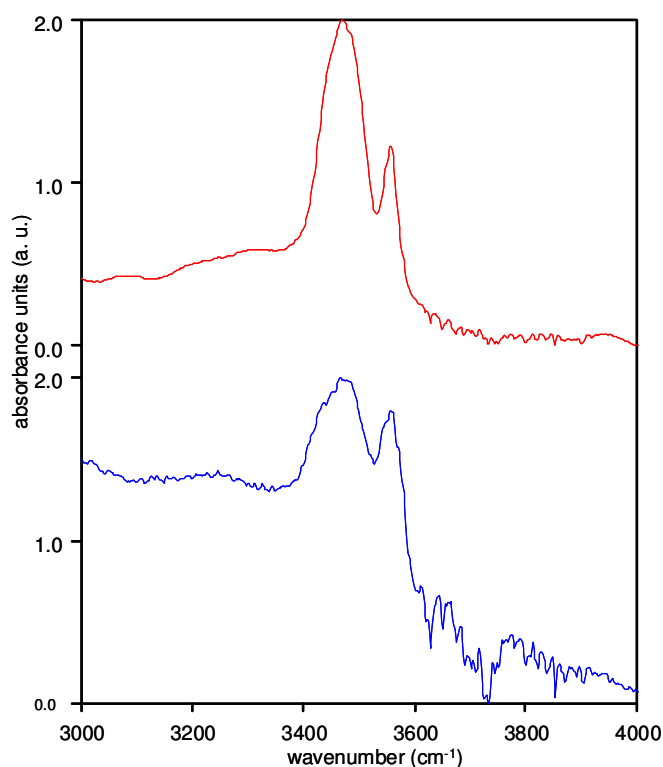


Figure 5. FTIR absorbance spectra on single crystals of  $\text{Er}_5(\text{BO}_3)_2\text{F}_9$  (top) and  $\text{Yb}_5(\text{BO}_3)_2\text{F}_9$  (bottom) in the range  $3000\text{-}4000 \text{ cm}^{-1}$ .

The single crystals, which were examined *via* IR spectroscopy, have been exposed to air and humidity and were not dried under high vacuum like the bulk material of

Yb<sub>5</sub>(BO<sub>3</sub>)<sub>2</sub>F<sub>9</sub>. Thus, the exchange of fluoride with OH-groups occurs due to hygroscopic alteration. In apatites, the exchange of hydroxyl and fluoride ions was previously observed and studied [35, 36].

### Raman spectroscopy

Raman spectra of single crystals of RE<sub>5</sub>(BO<sub>3</sub>)<sub>2</sub>F<sub>9</sub> (RE = Er, Yb) were measured without polarizers in the range 100 - 1600 cm<sup>-1</sup>, using a HORIBA LABRAM HR-800 confocal micro-spectrometer and a 785 nm diode laser. Laser focus and power on the sample surface was ~1 μm and ~10 mW, respectively. Depth resolution was ~4 μm, spectral resolution ~6 cm<sup>-1</sup>. Wavenumber accuracy of ~3 cm<sup>-1</sup> was achieved by regularly adjusting the zero-order position of the grating and checked by a Neon calibration lamp. Third order polynomial background subtraction, normalization and band fitting by Gauss-Lorentz functions were done by the LABSPEC 5 software (HORIBA). Some glue contamination cannot be excluded.

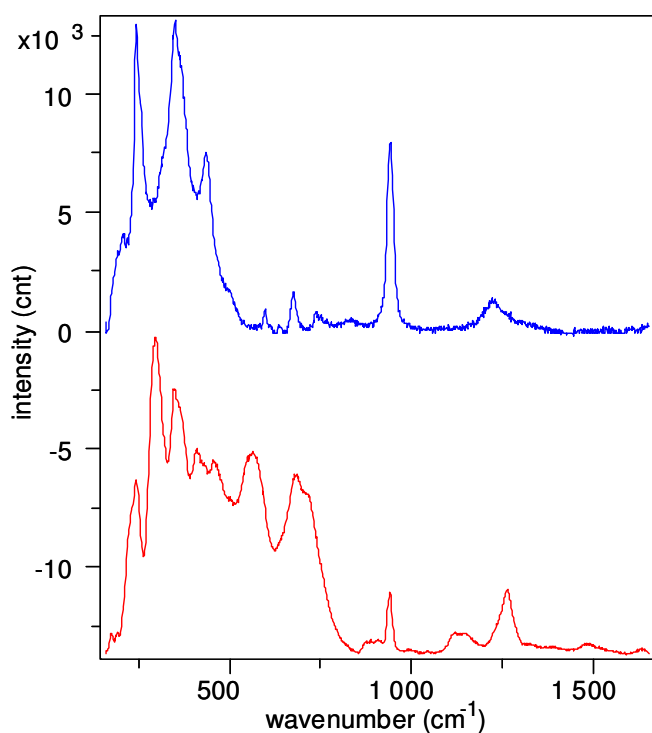


Figure 6. Raman-spectra on single crystals of Yb<sub>5</sub>(BO<sub>3</sub>)<sub>2</sub>F<sub>9</sub> (top) and Er<sub>5</sub>(BO<sub>3</sub>)<sub>2</sub>F<sub>9</sub> (bottom) in the range 100-1600 cm<sup>-1</sup>.

The Raman spectra of the isotopic compounds RE<sub>5</sub>(BO<sub>3</sub>)<sub>2</sub>F<sub>9</sub> (RE = Er, Yb) are quite similar with the most intense bands < 500 cm<sup>-1</sup> and the narrow, “isolated” band at ~940 cm<sup>-1</sup> (Figure 6). Above 1000 cm<sup>-1</sup>, one broad band for Yb<sub>5</sub>(BO<sub>3</sub>)<sub>2</sub>F<sub>9</sub> and several broader bands for Er<sub>5</sub>(BO<sub>3</sub>)<sub>2</sub>F<sub>9</sub> are observed. Bands around 900 cm<sup>-1</sup> in borates are usually assigned to stretching modes of BO<sub>4</sub>-tetrahedra whereas BO<sub>3</sub>-groups are expected > 1100 cm<sup>-1</sup> [4, 37 – 42]. However, in hydrated monoborates very intense bands at 882 and 501 cm<sup>-1</sup> were observed and assigned to symmetric stretching vibrations of the isolated BO<sub>3</sub>-groups [39]. The unusually large variation of B–O distances inside the BO<sub>3</sub>-groups (see above) might account for the comparatively low wavenumber and the large wavenumber range of these

bands. Bands < 500 cm<sup>-1</sup> can be assigned to bending and stretching vibrations of the isolated BO<sub>3</sub>-groups, RE–O, RE–F, F–O bonds, and lattice vibrations.

### Thermal behaviour of Yb<sub>5</sub>(BO<sub>3</sub>)<sub>2</sub>F<sub>9</sub>

*In situ* X-ray powder diffraction experiments were done on a STOE STADI P powder diffractometer [MoK<sub>α1</sub> radiation (λ = 71.073 pm)] with a computer controlled STOE furnace: The sample was enclosed in a silica capillary and heated from room temperature to 500 °C in 100 °C steps, and from 500 °C to 1100 °C in 50 °C steps. The heating rate was set to 40 °C/min. Afterwards, the sample was cooled down to 500 °C in 50 °C steps, and from 500 °C to room temperature in 100 °C steps (cooling rate: 50 °C/min). After each heating step, a diffraction pattern was recorded over the angular range 3° ≤ 2θ ≤ 40°. The temperature-dependent X-ray powder diffraction experiment on Yb<sub>5</sub>(BO<sub>3</sub>)<sub>2</sub>F<sub>9</sub> indicated a decomposition and subsequent phase changes of the decomposition products (Figure 7). Successive heating of Yb<sub>5</sub>(BO<sub>3</sub>)<sub>2</sub>F<sub>9</sub> in the range of 650-850 °C resulted in a decomposition into a mixture of π-YbBO<sub>3</sub> [43] and another still unidentified phase. Further heating led to a transformation of π-YbBO<sub>3</sub> into the high-temperature polymorph μ-YbBO<sub>3</sub> [43] in the range of 900-1100 °C. Additionally, reflections of YbF<sub>3</sub> and a formation of the silicate Yb<sub>2</sub>Si<sub>2</sub>O<sub>7</sub> [44] were observed. The latter was formed by a reaction with the silica capillary, which is known to happen occasionally. Subsequent cooling showed a complete retransformation into the low-temperature polymorph π-YbBO<sub>3</sub> below 500 °C. The formation and transformation of π-YbBO<sub>3</sub> into the high-temperature polymorph μ-YbBO<sub>3</sub> and back have been often observed in temperature-dependent X-ray powder diffraction experiments of ytterbium borates, e.g. with Yb<sub>3</sub>B<sub>5</sub>O<sub>12</sub> [9].

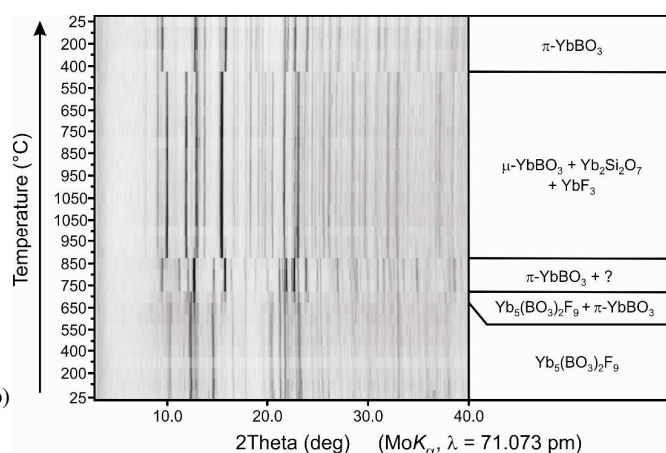


Figure 7. Temperature-dependent X-ray powder patterns, following the decomposition reaction of Yb<sub>5</sub>(BO<sub>3</sub>)<sub>2</sub>F<sub>9</sub>.

### Conclusions

The successful syntheses of Yb<sub>5</sub>(BO<sub>3</sub>)<sub>2</sub>F<sub>9</sub> (7.5 GPa) and the isotopic erbium fluoride borate Er<sub>5</sub>(BO<sub>3</sub>)<sub>2</sub>F<sub>9</sub> at a pressure of 3 GPa suggest a large formation region for these high pressure phases. The application of similar synthetic conditions to neighbouring rare-earth elements could lead to additional isotopic compounds and will be studied in the future. However, in the case of RE<sup>3+</sup> = Yb<sup>3+</sup>, experiments at higher pressures (10 GPa) resulted in the formation of an

apatite-structured compound, wherein all boron atoms showed a fourfold coordination [10].

## Acknowledgments

We thank Dr. Gunter Heymann for collecting the single-crystal data. Special thanks go to Christian Minke (LMU Munich) for the EDX analyses.

- [1] A. Haberer, H. Huppertz, *J. Solid State Chem.* **2009**, *182*, 888.
- [2] A. Haberer, H. Huppertz, *Solid State Sci.*, doi:10.1016/j.solidstatesciences.2009.12.017.
- [3] A. Haberer, R. Kaindl, H. Huppertz, *J. Solid State Chem.* **2010**, *183*, 471.
- [4] G. Corbel, R. Retoux, M. Leblanc, *J. Solid State Chem.* **1998**, *139*, 52.
- [5] H. Müller-Bunz, Th. Schleid, *Z. Anorg. Allg. Chem.* **2002**, *628*, 2750.
- [6] H. Huppertz, B. von der Eltz, *J. Am. Chem. Soc.* **2002**, *124*, 9376.
- [7] H. Huppertz, *Z. Naturforsch.* **2003**, *B58*, 278.
- [8] H. Huppertz, H. Emme, *J. Phys.: Condens. Matter* **2004**, *16*, 1283.
- [9] H. Emme, M. Valldor, R. Pöttgen, H. Huppertz, *Chem. Mater.* **2005**, *17*, 2707.
- [10] A. Haberer, H. Huppertz, unpublished results.
- [11] H. Huppertz, *Z. Kristallogr.* **2004**, *219*, 330.
- [12] R. E. Newnham, M. J. Redman, R. P. Santoro, *J. Am. Ceram. Soc.* **1963**, *46*, 253.
- [13] Z. Otwinowski, W. Minor, *Methods Enzymol.* **1997**, *276*, 307.
- [14] G. M. Sheldrick, *SHELXS-97 and SHELXL-97, Program suite for the solution and refinement of crystal structures*, **1997**, University of Göttingen, Göttingen, Germany.
- [15] G. M. Sheldrick, *Acta Crystallogr. A* **2008**, *64*, 112.
- [16] R. D. Shannon, *Acta Crystallogr.* **1976**, *A32*, 751.
- [17] A. Vegas, *Acta Crystallogr. B* **1977**, *33*, 3607.
- [18] H. Huppertz, *Z. Naturforsch. B* **2001**, *56*, 697.
- [19] R. Diehl, *Solid State Commun.* **1975**, *17*, 743.
- [20] A.S. Wills, *VaList Version 3.0.13*, **1998-2008**, University College London, UK. Program available from www.ccp14.ac.uk
- [21] I.D. Brown, D. Altermatt, *Acta Crystallogr. B* **1985**, *41*, 244.
- [22] N.E. Brese, M. O'Keeffe, *Acta Crystallogr. B* **1991**, *47*, 192.
- [23] R. Hoppe, S. Voigt, H. Glaum, J. Kissel, H. P. Müller, K. J. Bernet, *Less-Common Met.* **1989**, *156*, 105.
- [24] R. Hoppe, *Angew. Chem.* **1966**, *78*, 52-63; *Angew. Chem. Int. Ed. Engl.* **1966**, *5*, 95-106.
- [25] R. Hoppe, *Angew. Chem.* **1970**, *82*, 7-16; *Angew. Chem. Int. Ed. Engl.* **1970**, *9*, 25-34.
- [26] R. Hübenthal, *MAPLE (version 4), program for the calculation of MAPLE values*, **1993**, University of Gießen, Gießen (Germany).
- [27] H.R. Hoekstra, *Inorg. Chem.* **1966**, *5*, 754.
- [28] S.V. Berger, *Acta Crystallogr.* **1952**, *5*, 389.
- [29] A. Zalkin, D. H. Templeton, *J. Am. Chem. Soc.* **1953**, *75*, 2453.
- [30] E. Krausz, *Aust. J. Chem.* **1993**, *46*, 1041.
- [31] E. Krausz, *AOS News* **1998**, *12*, 21.
- [32] B. Henderson, G. F. Imbusch, *Optical Spectroscopy of Solids*, Oxford University Press, **1989**.
- [33] J.P. Laperches, P. Tarte, *Spectrochim. Acta* **1966**, *22*, 1201.
- [34] G. Heymann, K. Beyer, H. Huppertz, *Z. Naturforsch. B*, **2004**, *59*, 1200.
- [35] A. Knappwost, *Naturwiss.* **1959**, *46*, 555.
- [36] V. P. Orlovskii, S. P. Ionov, T. V. Belyaevskaya, S. M. Barinov, *Inorg. Mater.* **2002**, *38*, 182.
- [37] H. Emme, H. Huppertz, *Chem. Eur. J.* **2003**, *9*, 3623.
- [38] H. Huppertz, *J. Solid State Chem.*, **2004**, *177*, 3700.
- [39] L. Jun, X. Shuping, G. Shiyang, *Spectrochim. Acta A* **1995**, *51*, 519.
- [40] G. Chadeyron, M. El-Ghozzi, R. Mahiou, A. Arbus, J. C. Cousseins, *J. Solid State Chem.*, **1997**, *128*, 261.
- [41] J. C. Zhang, Y. H. Wang, X. Guo, *J. Lumin.* **2007**, *122-123*, 980.
- [42] G. Padmaja, P. Kistaiah, *J. Phys. Chem. A* **2009**, *113*, 2397.
- [43] W. F. Bradley, D. L. Graf, R. S. Roth, *Acta Crystallogr.* **1966**, *20*, 284.
- [44] Y. I. Smolin, Y. F. Shepelev, *Acta Crystallogr. B* **1970**, *26*, 484.

Received: ((will be filled in by the editorial staff))  
Published online: ((will be filled in by the editorial staff))

1  
2  
3  
4  
5  
6  
7  
8  
9  
10  
11  
12  
13  
14  
15  
16  
17  
18  
19  
20  
21  
22  
23  
24  
25  
26  
27  
28  
29  
30  
31  
32  
33  
34  
35  
36  
37  
38  
39  
40  
41  
42  
43  
44  
45  
46  
47  
48  
49  
50  
51  
52  
53  
54  
55  
56  
57  
58  
59  
60